



ARTICLE



Meta-analysis of human prediction error for incentives, perception, cognition, and action

Philip R. Corlett ^{1,2}✉, Jessica A. Mollick^{1,2} and Hedy Kober ¹✉

© The Author(s), under exclusive licence to American College of Neuropsychopharmacology 2022

Prediction errors (PEs) are a keystone for computational neuroscience. Their association with midbrain neural firing has been confirmed across species and has inspired the construction of artificial intelligence that can outperform humans. However, there is still much to learn. Here, we leverage the wealth of human PE data acquired in the functional neuroimaging setting in service of a deeper understanding, using an MKDA (multi-level kernel-based density) meta-analysis. Studies were identified with Google Scholar, and we included studies with healthy adult participants that reported activation coordinates corresponding to PEs published between 1999–2018. Across 264 PE studies that have focused on reward, punishment, action, cognition, and perception, consistent with domain-general theoretical models of prediction error we found midbrain PE signals during cognitive and reward learning tasks, and an insula PE signal for perceptual, social, cognitive, and reward prediction errors. There was evidence for domain-specific error signals—in the visual hierarchy during visual perception, and the dorsomedial prefrontal cortex during social inference. We assessed bias following prior neuroimaging meta-analyses and used family-wise error correction for multiple comparisons. This organization of computation by region will be invaluable in building and testing mechanistic models of cognitive function and dysfunction in machines, humans, and other animals. Limitations include small sample sizes and ROI masking in some included studies, which we addressed by weighting each study by sample size, and directly comparing whole brain vs. ROI-based results.

Neuropsychopharmacology (2022) 47:1339–1349; <https://doi.org/10.1038/s41386-021-01264-3>

INTRODUCTION

The reward prediction error (PE) signal in primate midbrain codes a mismatch between expected and experienced reward. It updates value expectations and drives action selection according to reinforcement learning theory [1]. It has been measured invasively in rodents [2, 3], primates [1], and humans [4], and studied with functional magnetic resonance imaging (fMRI) in humans [5]. It has been causally implicated in learning with optogenetics [6].

Recently the scope of PE has broadened to fMRI studies of perceptual [7], social [8], linguistic [9], and causal inferences [10]. We conducted a quantitative meta-analysis of studies of reward PE and PE cast more broadly. We sought to determine whether PEs invoked as mechanisms across domains of processing share underlying neural substrates, or rather, each domain implements its own specific PE.

We integrate findings from multiple independent studies of PE [11]. Functional imaging studies are expensive so sample sizes are often limited, which limits statistical power to detect true responses, and undermines confidence in cognitive neuroscience [11]. By summarizing across reported PE signals and weighting the contribution of each study by its quality [11], we learn how varieties of PE are instantiated in the human brain.

METHODS

Search strategy and study selection

The Preferred Reporting Items for Systematic Reviews and Meta-Analysis (PRISMA) system guided our search and selection (see Figure S1). We searched Google Scholar, with the following terms: (1) “predic* AND error* AND (fMRI OR imaging OR neuroimaging) AND (learning OR conditioning)”, and (2) “reinforcement AND (fMRI OR imaging OR neuroimaging) AND (learning OR conditioning).” Separate searches were conducted for each year between 1999–2018, with publication date restricted to December 2018 at the latest. We first reviewed abstracts, and excluded those that were irrelevant (e.g., animal data only, reviews, etc). Full text papers were then read by two authors (JAM & PRC) to determine final inclusion. Next, we selected 13 of the most highly-cited included papers, searched for papers that cited them (i.e., forward search), and examined those papers for inclusion. We also searched through reference sections of previously published meta-analyses, reviews, and papers identified by searching Neurosynth (Neurosynth.org) for the terms (“prediction AND error” and “reinforcement AND learning”).

38,831 abstracts were identified: 26,106 from searches and 12,725 from other sources.

After removing duplicates, 24,751 abstracts were reviewed, and 574 full-text papers were evaluated for inclusion. Of those, 263 papers were included in analyses, contributing 464 independent contrasts, and representing 6,454 participants.

Only published, peer-reviewed, original research articles were considered. Included studies met the following criteria: (1) Human adult participants 18–65; (2) They employed fMRI; (3) They provided Talairach

¹Department of Psychiatry, Yale University, New Haven, CT, USA. ²These authors contributed equally: Philip R. Corlett, Jessica A. Mollick. ✉email: philip.corlett@yale.edu; hedy.kober@yale.edu

Table 1. Prediction error coding scheme.

| | |
|-----------------------------|---|
| Outcome type | |
| Primary reward/punishment | PEs induced by primary rewards such as juice, water, or food; primary punishment PEs involved a primary punishment such as shock or pain. |
| Secondary reward/punishment | PEs for secondary reward/punishment if they involved a monetary or points outcome |
| Social | Social PEs were engendered by events involving other people, e.g. surprising changes in their attributes or behavior. |
| Specific outcome | |
| Money | The outcome was a monetary reward. |
| Points | The outcome was a points reward. |
| PE type | |
| Typical | “Typical” PEs corresponded to reward and punishment prediction errors. |
| Perceptual | “Perceptual” PEs involved an unexpected perceptual event without an explicit reward or punishment. |
| Cognitive | “Cognitive” PEs involved violations of expectations based on beliefs, except beliefs about rewards (whose violations were coded “Typical”). |
| Signed/Unsigned | |
| | PEs were “signed” if they (1) represented brain activity aligned with a computational model where PE increased for outcomes that were better than expected and decreased for outcomes that were worse than expected, or (2) compared outcomes that were specifically better or worse than expected (vs. expected outcomes). |
| | PEs were “unsigned” if they (1) represented brain activity that corresponded to an unsigned parameter from a computational model (including Pearce-Hall prediction errors, belief violations from Bayesian models, KL divergence), or |
| | (2) compared violations of beliefs or expectations (vs. non violation), or |
| | (3) compared both better than expected and worse than expected outcomes (vs. expected outcomes). |
| Instrumental/Pavlovian | |
| | “Pavlovian” tasks involved passively learning associations between cues and rewards that were not contingent on participant actions. |
| | “Instrumental” tasks involved responses which engendered outcomes. |
| Appetitive/aversive | |
| | “Appetitive” outcomes corresponded to positively-valenced outcomes such as primary rewards, secondary monetary rewards, points, or positive feedback. |
| | “Aversive” outcomes corresponded to negatively-valenced outcomes such as pain, shock, negative feedback, social rejection, aversive taste, or aversive emotional pictures. |
| | Coordinates were coded as “both” if they involved both appetitive and aversive outcomes, and “neither” if they did not involve a positively- or negatively-valenced outcome. |
| ROI/whole brain | |
| | Coordinates were coded as “ROI” if they represented a region-of-interest and/or small-volume corrected analysis. |
| | Coordinates were coded as “whole brain” if analyses were conducted and/or corrected across the entire brain. |

or Montreal Neurological Institute (MNI) coordinates; (5) They used image subtraction or parametric modeling (using computational model parameters) to determine PE activation foci.

In the absence of PE, we excluded studies that focused on the anticipation of reward or punishment, extinction, subjective value, or correlations with learning rate parameters. We excluded papers with clinical groups; unless data from healthy comparison participants were reported separately. We excluded studies of drug administration, including placebo, since it may be PE mediated [12]. We excluded studies of genetic polymorphisms effects on PE.

Data extraction and reduction

For each included study we extracted the following information: N (number of participants contributing to each reported coordinate), xyz coordinate for each significant reported activation, coordinate system (Talairach or MNI), whether derived from a region of interest (ROI) or whole brain analyses, and whether statistical analyses employed a random/mixed or fixed effects model. Further, we coded several fields of meta-data, including: (1) whether PE was engendered by a primary or secondary reward; (2) the specific type of outcome (e.g., social, money, points, feedback); (3) the type of computational model (e.g., Bayesian,

temporal difference); (4) whether PE was positive (corresponding to an unexpected occurrence of reward or punishment), or negative (corresponding to an unexpected omission of reward or punishment); (4) whether PE was signed or unsigned; (5) whether PE was calculated at the time of the cue or during the outcome; (6) whether the task involved instrumental or Pavlovian conditioning; (7) whether the study involved an appetitive or an aversive outcome; (8a) PE type: typical reward prediction error, or atypical; prediction error capturing a violation of beliefs; and (8b) atypical PEs were further coded as: cognitive (if expectations based on beliefs were violated, but not beliefs about rewards), effort (if expectations based on physical or cognitive effort were violated), fictive (PE to an event that could have but did not occur or a choice that was not taken), risk (PE regarding the reward variance or its square root, standard deviation), and perceptual PEs (generated by unexpected perceptual events without explicit reward or punishment). All information was entered by one researcher and checked by the second researcher; any disagreements were discussed and resolved. Further details on the coding scheme for PEs are included in Table 1 and in the supplementary materials (study coding criteria, page 15). Coordinates reported in Talairach space were converted to MNI space using the Tal2MNI algorithm implemented in Matlab (<http://imaging.mrc-cbu.cam.ac.uk/imaging/MniTalairach>).

All Prediction Errors

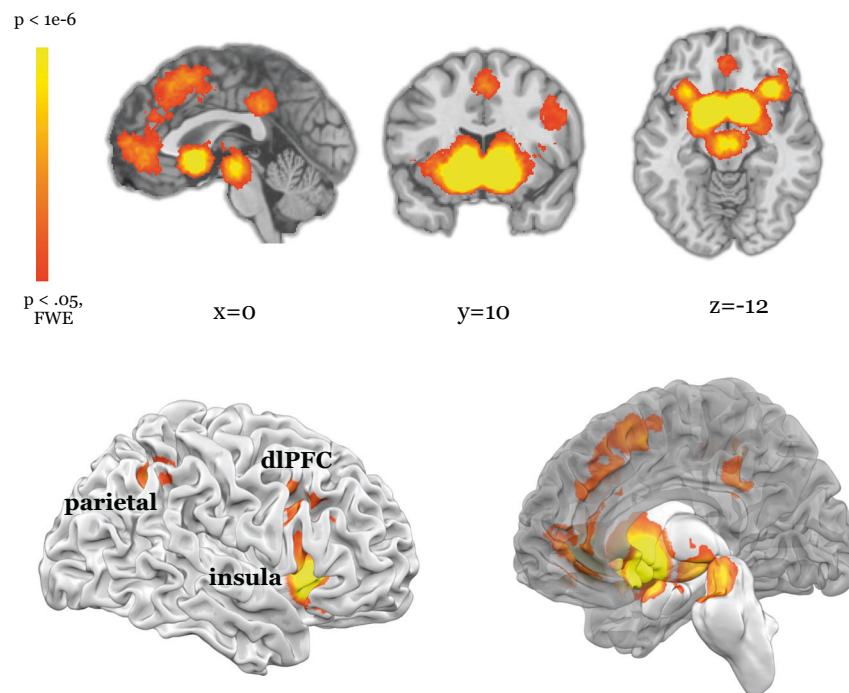


Fig. 1 Prediction error brain regions across studies. PE signals were found in the midbrain, striatum, thalamus, insula, claustrum, dorsomedial prefrontal cortex, ventrolateral PFC, dorsolateral prefrontal cortex (dlPFC), parietal cortex, precuneus, orbitofrontal cortex, occipital cortex, and anterior cingulate.

Statistical analysis

We used Multilevel Kernel Density Analysis (MKDA) to determine the distribution of peak coordinates [11]. Coordinates from each included contrast were plotted on the standard brain, then convolved with a 10 mm spherical kernel to create a map of voxels within 10 mm of the reported peak. This resulted in a “Contrast Indicator Map” (CIM), marked with a value of 1 for voxels within the kernel, indicating activation near this voxel, or a value of 0 for voxels outside of the kernel, indicating no activation near this voxel. Next, a density map was obtained by taking a weighted average of the CIMs, whereby weights are the square root of the sample size for each contrast, weighing larger studies more heavily. In line with prior meta-analyses, studies that used fixed effects analyses would be down-weighted (0.75); however, none of the included studies employed fixed effects analyses. This created an interpretable meta-analytic statistic (P) at each voxel, representing the weighed proportion of contrasts that activate within 10 mm of each voxel. These results were then thresholded using Monte–Carlo (MC) simulation: we compared the meta-analytic statistic (P) with a null-hypothesis density (P_0) estimated via simulation. The null hypothesis was a uniform random distribution of peaks within each contrast in the gray-matter mask of the standard brain. For each CIM, we identified contiguous activation clusters of suprathreshold voxels. In each of 5000 MC iterations, the spatial location of the activation clusters was selected at random within a gray-matter mask. After each MC iteration, the maximum cross-density statistic (P) over the whole brain was saved. To threshold the images, we then derived a critical Familywise Error (FWE) rate by determining the weighted cross-density statistic (P) that exceeds the whole brain maximum in 95% of the MC maps, controlling for false positives at $p < 0.05$ corrected. After each MC iteration, the largest cluster of contiguous voxels was saved, and we set a cluster extent threshold at the 95% percentile across iterations, following “cluster extent-based” multiple comparison correction [13]. Our results represent (1) Meta analysis across all included studies; (2) Meta-analyses across subsets of included contrasts (e.g., those coded as [signed PEs]); (3) Meta-contrasts that compare subsets of contrasts (e.g., [appetitive > aversive]); and (4) formal conjunctions of separate meta-analytic maps (e.g., [signed and unsigned prediction error]). Identical thresholding procedures were applied across these analyses: first, images were thresholded at a voxel-wise threshold of $p < 0.001$, and then we

thresholded them with a cluster extent threshold at a level of $p < 0.05$, FWE, determined with the MC procedure.

We created conjunction images using the minimum statistic method [14] with the weighted cross-density statistic (P). Each individual map contributing to the conjunction was independently thresholded at a level of $p < 0.05$, FWE using bootstrapping. Then, we calculated a formal conjunction across independently thresholded images. That is, voxels were included in the conjunction image only if activity exceeded the corrected threshold in all of the contributing maps. The conjunction map was thresholded with the minimum cluster threshold that exceeded $p < 0.05$, FWE. Conjunction analyses license conclusions about the voxels shared by particular types of PE. If PEs across domains share voxels we inferred that they share an underlying circuitry comprising those voxels. If this circuitry was more consistently engaged for one type of PE than the others, we inferred that this type of PE taxed the circuitry more strongly. We believe this because the magnitude of PE activity typically correlates with the extent of behavioral learning and belief change. Overall, we aimed to delineate the shared and unique circuitry underlying different domains of PE.

RESULTS

Omnibus contrast

Across all 464 contrasts from 263 included papers we found PE signals in the midbrain, dorsal and ventral striatum, thalamus, amygdala, insula, claustrum, dorsolateral prefrontal cortex (dlPFC), ventrolateral PFC (vlPFC), parietal cortex, precuneus, orbitofrontal and medial prefrontal cortex, occipital cortex, and posterior and anterior cingulate (Fig. 1, Table S1).

Primary versus secondary rewards

We examined PEs for primary reinforcers (like juice, Fig. S2A, Table S2A) compared to secondary reinforcers (like money, Fig. S2B, Table S2B). If these are coded relative to some ‘common currency’, they ought to share processing loci [15]. On the other hand, motivational state and degree of familiarity may generate unique PE loci for primary versus secondary rewards.

Conjunction analysis revealed that PE for both primary and secondary rewards engaged both dorsal and ventral striatum, midbrain, and insula and vIPFC (Fig. S2D, Table S2E). This is consistent with a “common currency” account.

However, when we compared them, primary rewards more consistently induced PEs in the dorsal striatum, amygdala, parahippocampal gyrus, claustrum and insula, anterior cingulate, vIPFC, dmPFC, and supplementary motor area than secondary (Fig. S2C, Table S2C). Secondary rewards more consistently engaged the ventral striatum and subgenual cingulate (Fig. S2C, Table S2D).

Further, PEs for points more commonly engaged the ventral striatum, thalamus, medial PFC, and subgenual cingulate than those for money (Figure S7, Table S11A), while regions that were more engaged with money than points included the subgenual cingulate extending into OFC, and distinct regions of dorsal and ventral striatum (Fig. S7, Table S11B).

Appetitive and aversive

We examined aversive and reward PEs in human fMRI studies. Brain regions encoding appetitive PE included vIPFC, both dorsal and ventral striatum, amygdala, thalamus, midbrain, bilateral insula, medial PFC (mPFC), anterior and posterior cingulate, and vIPFC (Fig. S3A, Table S3A). Aversive PEs were encoded in insula, claustrum, vIPFC, supplementary motor area, dorsomedial PFC (dmPFC), precuneus, both dorsal and ventral striatum, midbrain, amygdala, parahippocampal gyrus, thalamus, and subgenual cingulate (Fig. S3B, Table S3B).

Conjunction analysis revealed both appetitive and aversive PEs engaged the midbrain and dorsal and ventral striatum, amygdala, parahippocampal gyrus, insula, cingulate, claustrum, and vIPFC (Fig. S3D, Table S3E). However, contrasting appetitive with aversive PE, we found more consistent appetitive PE responses in dmPFC, mPFC, subgenual cingulate, posterior cingulate, parietal lobe, and both dorsal and ventral striatum (Fig. S3C, Table S3C). There was more activity for aversive vs. appetitive PEs in the vIPFC, insula, claustrum, dmPFC, anterior cingulate, a more posterior region of the midbrain, as well as distinct regions of dorsal and ventral striatum, amygdala, hippocampus, and thalamus. (Fig. S3C, Table S3D).

Perceptual and cognitive prediction error

We tested whether regions of the dopamine system also underpin learning perception and cognition. Computing a conjunction across typical reward, perceptual, and cognitive PEs revealed PE signals in the ventral striatum, dorsal striatum, pallidum, insula, and vIPFC (Fig. 2D, Table S4D).

Predictive processing models of the mind and brain posit a cost function for state transitions (rather than value). Under predictive processing, sensory hierarchies, like the visual system, ought to compute and exhibit PEs. Indeed, this is what we observe: PEs spanning the visual cortical hierarchy (Fig. 2C, Table S4B). However, it is unclear whether reward and perceptual prediction errors are computed by the same systems. Some theories suggest they are identical [16]. To test for such overlap, we computed a formal conjunction of perceptual and typical reward PEs (Fig. S6A, Table S4D). This revealed overlapping activity in the dorsal and ventral striatum, thalamus, and insula.

Instrumental and Pavlovian prediction error

Organisms learn passively from the environment (Pavlovian), and actively from the consequences of their actions (Instrumental) [17]. Instrumental PEs engaged the dorsal and ventral striatum, insula, midbrain, and frontal regions including vIPFC, dmPFC, mPFC, anterior and posterior cingulate, parietal regions, and occipital gyrus (Fig. 3A, Table S5A). Pavlovian PEs engaged dorsal and ventral striatum, midbrain, anterior cingulate, amygdala, thalamus, insula, and vIPFC extending into OFC (Fig. 3B, Table S5B). The contrast of instrumental PEs vs. Pavlovian PEs revealed that instrumental PEs were associated with activity in dorsal and ventral striatum, anterior cingulate,

posterior cingulate, dorsomedial PFC, frontal eye field and parietal cortex (Fig. 5C, Table S6C). Pavlovian PEs were more likely to be associated with activity in amygdala, parahippocampal gyrus, putamen, insula, thalamus, dlPFC, dmPFC, precentral gyrus, a distinct region of cingulate gyrus, and temporal and occipital regions (Fig. 3C, Table S5D). A conjunction revealed dorsal and ventral striatum, pallidum, midbrain and insula (Fig. 3D, Table S5E). There were more consistent Pavlovian PEs in the OFC. This is congruent with preclinical data, wherein rodent OFC lesions impair updating of stimulus-outcome associations, but not instrumental learning [18]. However, there may be dissociable learning mechanisms within OFC [19]. It appears medial OFC was more consistently engaged by instrumental PE, and lateral more consistently engaged by Pavlovian PE. This aligns with rodent work that suggests lateral OFC lesions impair Pavlovian (but not instrumental) learning [20], and medial lesions impair Instrumental learning [21].

Furthermore, there was also substantial overlap between Instrumental versus Pavlovian learning and appetitive versus aversive PEs (Fig. S8, Table S12). This may speak to the relative importance of positive versus negative reinforcement in action selection. However, we favor a more mundane explanation: The apparent similarity between instrumental/appetitive and Pavlovian/aversive PEs may be a function of prevailing experimental trends: human functional neuroimaging studies of instrumental learning rarely employ negative outcomes. Pavlovian conditioning studies in human participants often employ aversive outcomes. Using a chi-squared test, we found that valence labels (appetitive and aversive) were differentially related to the instrumental and Pavlovian labels ($\chi^2 = 11.77$, $p = 0.0006$). Specifically, the odds of Instrumental studies being appetitive compared to Pavlovian studies were 3.48–1 [95% CI = 1.72,7.10; relative risk: 1.55, 95% CI = 1.16,2.08].

Active inference?

Some predictive coding accounts posit a PE minimization mechanism for one’s actions and their impact upon perception—in this way dopaminergic PEs impact perception [16]. Recent preclinical data support this idea [22]. Active inference accounts suggest that actions that minimize PEs are selected [23]. The conjunction of Pavlovian, Instrumental, and Perceptual PE thus defines possible circuits for active inference. This analysis revealed claustrum, bilateral insula extending into OFC, and dorsal and ventral striatum (Fig. S5, Table S9).

Precision-weighted and social prediction error

Some accounts center on the precision of PE: they contribute to learning to the extent that they are reliable. We compare and contrast the circuits underlying PEs with and without precision-weighting (Fig. S4). In formal associative learning theory, there are models that track signed PEs—PEs that have a positive or negative sign – and others that track unsigned PEs, which may increase cue processing, associability, and learning about stimuli with unpredictable consequences [24] or decrease them, focusing instead on stimuli that serve as reliable predictors [25]. None of the papers in our meta-analysis fell in this latter category. All the papers that employed unsigned PE modeled errors to increase learning rates; thus, we consider them precision-weighted PE in the predictive processing sense (i.e., that they weight the impact of PE by its variability).

Both signed and unsigned PEs were associated with activity in the midbrain, dorsal and ventral striatum, insula, supplementary motor area, and frontal eye field (Fig. S3D, Table S8E). However, comparing signed to unsigned PEs revealed more activity in dorsal and ventral striatum, pallidum, medial PFC, and anterior and posterior cingulate for signed PEs, while unsigned PEs were associated with more consistent activations in cerebellum, dlPFC, dmPFC and a distinct cingulate region, supplementary motor area, supramarginal gyrus, parietal regions, middle temporal gyrus, claustrum, and disparate regions of insula compared to signed PEs (Fig. S3C, Table S8C).

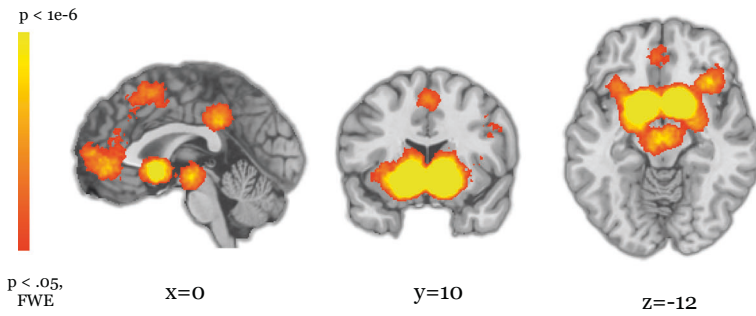
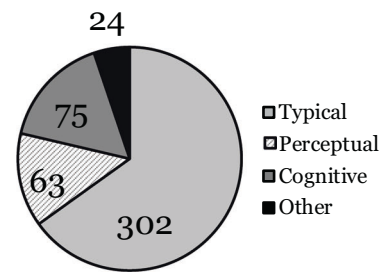
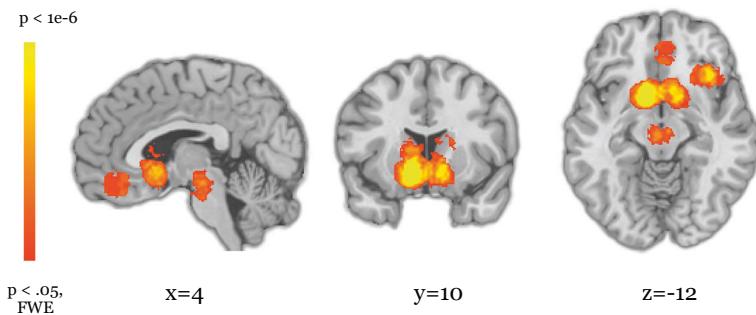
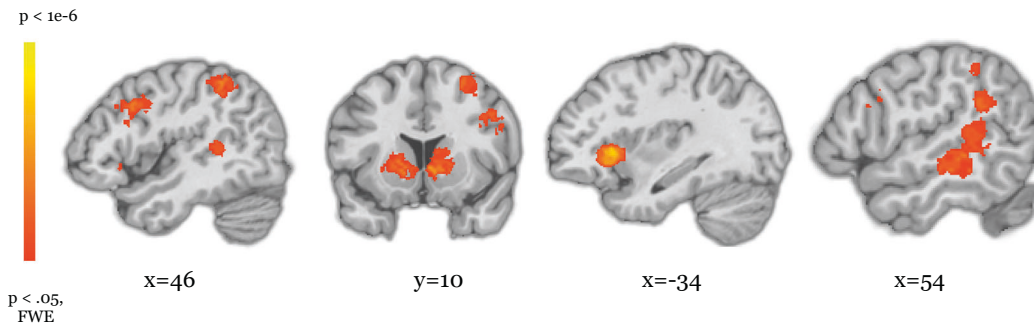
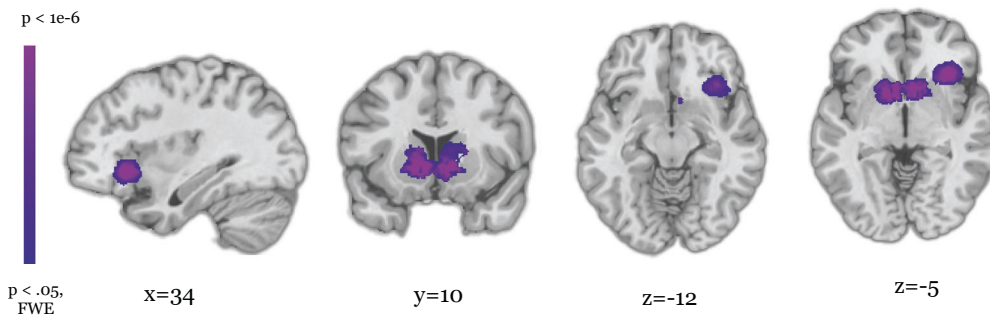
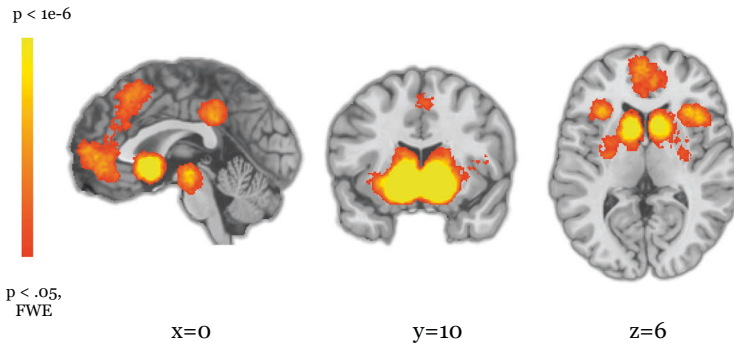
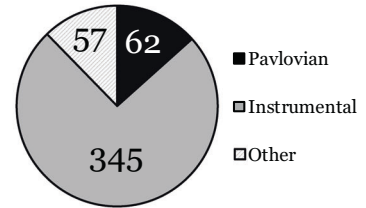
A. Typical PE**Contrast counts****B. Cognitive PE****C. Perceptual PE****D. Typical, Perceptual & Cognitive PEs**

Fig. 2 Typical, perceptual, and cognitive prediction errors. **A** Typical PE engaged anterior cingulate, ventral and dorsomedial PFC, posterior cingulate, striatum, midbrain, and insula. **B** Cognitive PE engaged dorsomedial and ventromedial PFC, striatum, midbrain, and ventrolateral PFC. **C** Perceptual PE engaged dorsolateral PFC, parietal cortex, striatum, and middle temporal gyrus, superior temporal gyrus, supramarginal gyrus, and parietal lobe. **D** A conjunction across typical reward, perceptual, and cognitive PEs revealed PE signals in regions including the ventral and dorsal striatum, pallidum, insula, and ventrolateral PFC.

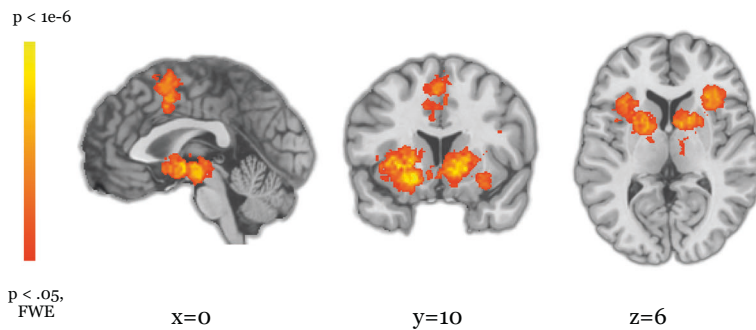
A. Instrumental PE



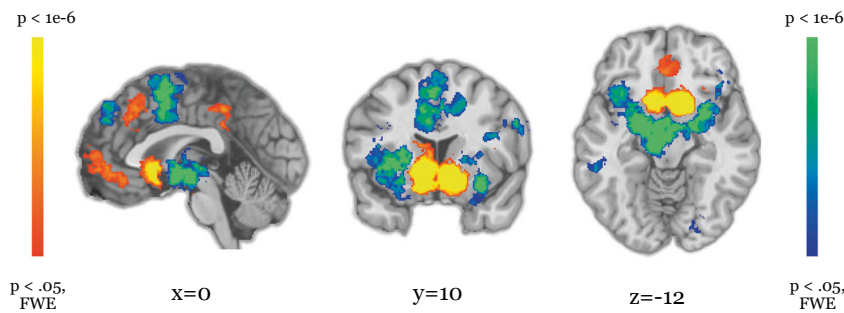
Contrast counts



B. Pavlovian PE



C. Instrumental > Pavlovian PE



D. Instrumental & Pavlovian Conjunction

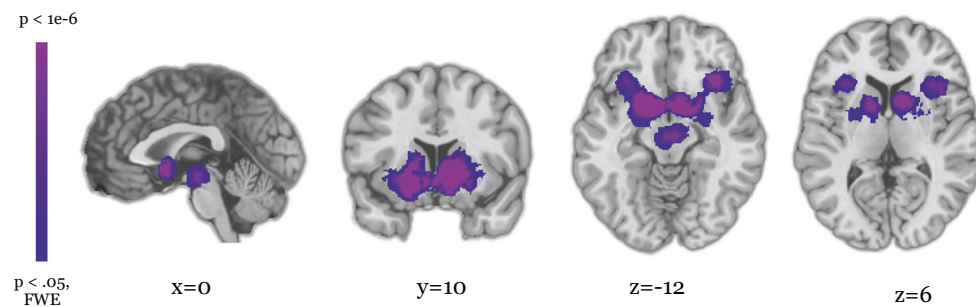


Fig. 3 Instrumental and Pavlovian prediction errors. **A** Instrumental PEs engaged the dorsal and ventral striatum, insula, midbrain, and frontal regions including ventromedial and dorsomedial PFC, ventrolateral PFC, anterior and posterior cingulate, and parietal regions. **B** Pavlovian PEs engaged dorsal and ventral striatum, midbrain, anterior cingulate, amygdala, thalamus, parietal regions, insula, and inferior frontal gyrus. **C** The contrast of instrumental PEs vs. Pavlovian PEs revealed that instrumental PEs were associated with activity in ventral striatum, anterior cingulate cortex, posterior cingulate, midbrain, dorsomedial PFC, dorsolateral PFC, precentral gyrus, precuneus, and parietal cortex (orange). Pavlovian PEs were more likely to be associated with activity in amygdala, putamen, insula, thalamus, a distinct region of cingulate gyrus, and temporal and occipital regions (blue). **D** A conjunction revealed striatum, midbrain, insula, and parietal regions.

These findings may also inform the mechanisms of social inference. At issue is whether there are dedicated, informationally encapsulated, social modules in the mind and brain [26]. Alternatively, social inference may, through phylogeny, have co-opted general precision-weighted inference mechanisms. We computed the intersection between regions evincing PEs during social tasks, and those reflecting non-social PEs, and in particular precision-weighted PEs. We found extensive overlap (Fig. 4D, Table S6C). Dorsal and ventral striatum, pallidum, vIPFC, orbitofrontal cortex, and insula appeared in the intersection between social and precision-weighted non-social PEs.

We also found relatively more activation for social PEs than other non-social PEs in cingulate, dmPFC, and ventromedial and orbitofrontal PFC (Fig. 4C). Notably, these regions are not unique to social processes or to social PEs [27, 28], although recent single-unit recordings in human dmPFC did show selectivity for PE about others' beliefs, there were neurons selective for sensory PEs, and others sensitive to both [29]. Dorsal and ventral striatum, anterior and posterior cingulate, a distinct region of mPFC, thalamus, left insula, midbrain, and parahippocampal gyrus were more engaged for non-social PE than social PE.

Midbrain PEs

We employed FWE cluster extent thresholding. It affords sensitivity to weak and diffuse signals, but has poor spatial specificity, which is problematic for smaller regions like the midbrain. We observed midbrain PE signals in our omnibus analysis, as well as for reward PE, and cognitive PE, even with this thresholding approach. However, when we focus on the midbrain and relax the cluster extent threshold, we observe midbrain PE responses for perceptual and social tasks (Fig. S8A, Fig. S9A).

Regions of interest vs. whole brain analyses

Limiting analyses to a-priori regions of interest (ROIs) is common in functional neuroimaging. In PE studies, masking often focuses on striatum and midbrain. There is nothing erroneous about this approach, however, it runs the risk of the Drunkards Search Principle—people search where it is easiest to look (e.g., reasonably, where others have looked). Whilst a-priori preclinical data support searching for reward PEs in the striatum, doing so may have led our field to ignore other sources of reward PE in the human brain. To explore this possibility, we compared activations from contrasts that employed a-priori ROIs with those that did not. Results from whole brain contrasts consistently reported PE signals in the dlPFC, mPFC, parietal, and visual cortices more so than studies that employed ROI masks that were often limited to the basal ganglia and midbrain (Fig. 5A, Fig. 5B, Table S10). A contrast comparing PEs from whole brain compared to ROI analyses showed widespread cortical and subcortical regions, including medial and lateral PFC, insula, parietal regions, and temporal and occipital cortex (Fig. 5C). We further assessed reporting bias in terms of number of reported foci as a function of sample size (Fig. S11), but note that our MKDA approach uses contrast as a unit of analysis, weighted by sample size, and is less likely to be distorted by studies with larger numbers of foci.

DISCUSSION

We conducted the most comprehensive meta-analysis of fMRI studies of PE to date. Previous meta-analyses examined signed and unsigned PEs [30], Pavlovian and instrumental learning [5, 31, 32], as well as outcome type and valence [5, 32]. We consider all of these tasks and more, concurrently, and include more studies.

Our conjunction analyses (Figs. 2D, 3D, 4D, purple) suggest a core circuit that processes PE across domains incorporating dorsal and ventral striatum, and insula. We conceptually replicate Sharpe and colleagues [33], wherein midbrain dopamine neurons respond to violations of causal and perceptual expectation. We

observed these signals in the striatum, particularly when we examined the intersection between Pavlovian, Instrumental and perceptual PE signals. Consistent with predictive processing accounts of vision [34, 35]—we also observed perceptual PE signals spanning the visual processing hierarchy.

There appeared to be regionally compartmentalized PEs for primary and secondary rewards. Primary rewards elicited PEs in the dorsal striatum and amygdala, while secondary reward PEs were in ventral striatum. This is consistent with the representational transition that occurs with learning [36]. We also found separable PEs for valence domains: caudal regions of the caudate-putamen are involved in the learning of safety signals and avoidance learning [37–39], more anterior striatum is selective for rewards, while more posterior is selective for losses [40]. We found posterior midbrain aversive PE, consistent with preclinical findings that dopamine neurons—which respond to negative valence—are located more posteriorly in the midbrain and project to medial prefrontal regions [41]. Additionally, we found both appetitive and aversive PEs in the amygdala, consistent with animal studies [42–47]. The presence of both appetitive and aversive PE signals in the amygdala is consistent with its expanding role regulating learning based on surprise and uncertainty [48] rather than fear per se.

Perhaps conspicuous in its absence, given preclinical work, is the hippocampus, which is often held to be a nexus for reward PE, memory PE, and perceptual PE [49]. This may be because the hippocampus is constantly and commonly engaged throughout task performance. Its PEs may not be resolved by the sluggish BOLD response, which is based on local field potentials and may represent the projections into a region (and therefore the striatal PE signals we observed may be the culmination of the processing in CA1, CA3, and subiculum). Furthermore, we have only recently been able to image subfields of the hippocampus (with higher field strengths and more rapid sequences); as higher resolution PE papers accrue we will revisit the meta-analysis of PEs.

Precision weighting of PE has been increasingly emphasized, wherein PEs are accommodated or assimilated depending on their inverse variance. The core PE circuit seems to deal in precision-weighted as well as signed PE (Fig. 2D, Fig. S3). The human insula has consistently been implicated in precision weighting of reward [50–52] and perceptual PEs [53]. We confirmed these associations.

The extensive overlap between precision weighted PEs (across domains) and social PEs (a specific domain, Fig. 4D) is consistent with the idea that social and non-social inferences share underlying cognitive and neural machinery. A recent study observed overlap between unsigned PE and social conformity in the same participants—notably in the anterior insular cortex, as we observed [54]. However, multivoxel pattern analyses (MVPA) of the same data suggested independent voxels coded unsigned reward PEs and social conformity [54]. It is apparent from simulations that univariate and MVPA are sensitive to different data features [55]. MVPA is sensitive to voxel level variability even when the same linear relationship is present in all voxels [55], and it is insensitive to variability in mean activation across a region [55]. Thus, MVPA is not necessarily the golden-road to inferences about computation, and, furthermore, the same computational model ought to have been applied to the reinforcement learning and social conformity data, whilst exploring their shared and unique underlying computational architecture. We take this approach, centering PE across social and non-social studies. Our approach and results are more consistent with the univariate analysis—suggesting a shared focus on social and precision-weighted PE in the anterior insula and thus, a domain-general account of social inference.

However, the social vs. non-social PE contrast revealed regions that were more consistently engaged by social PEs, but also somewhat engaged by reward PEs more broadly (Fig. 7C). To establish specificity of social functions, Lockwood et al argue there must be dissociation between social and non-social in algorithm or implementation, and domain-general processes must be ruled

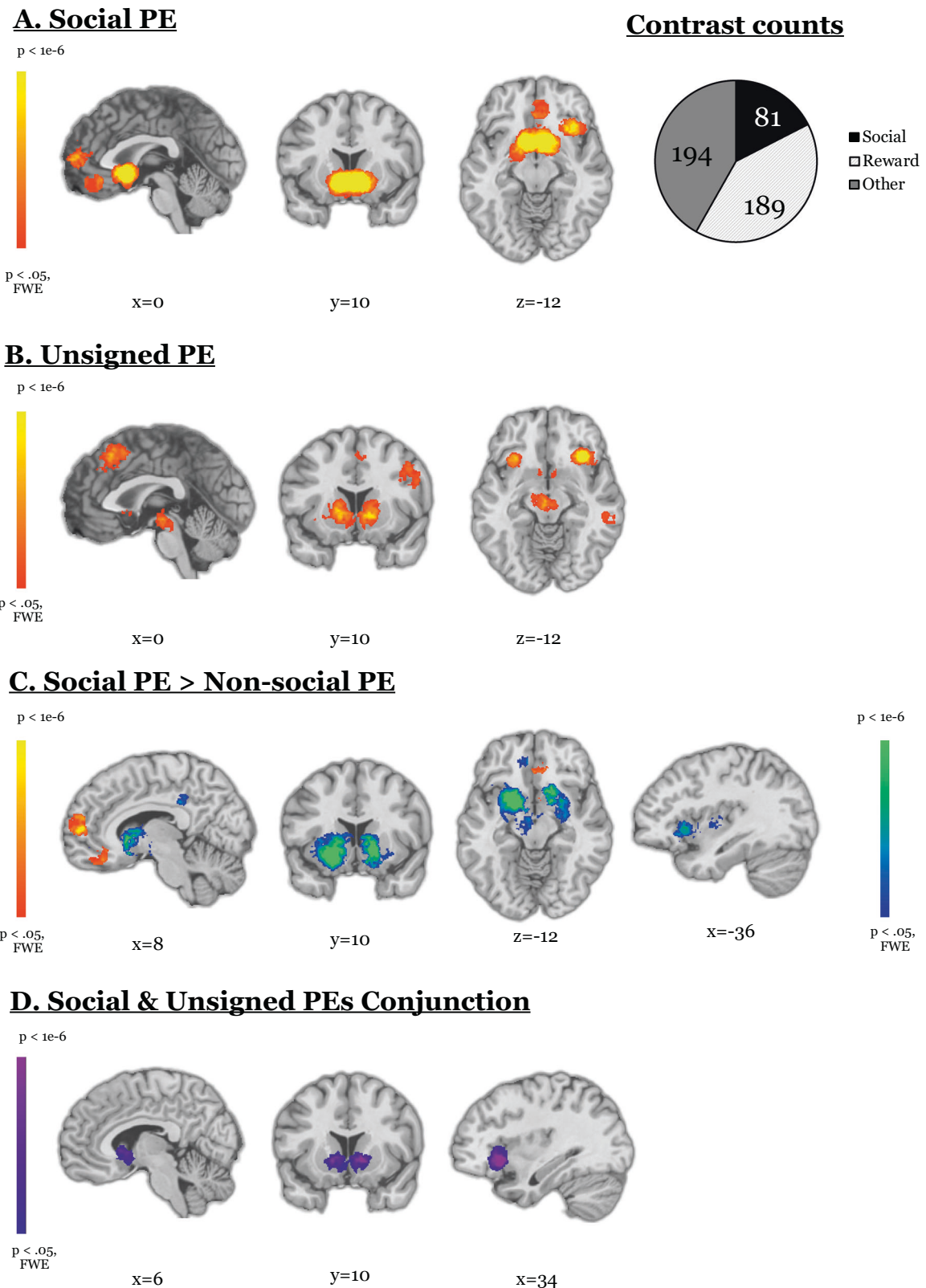
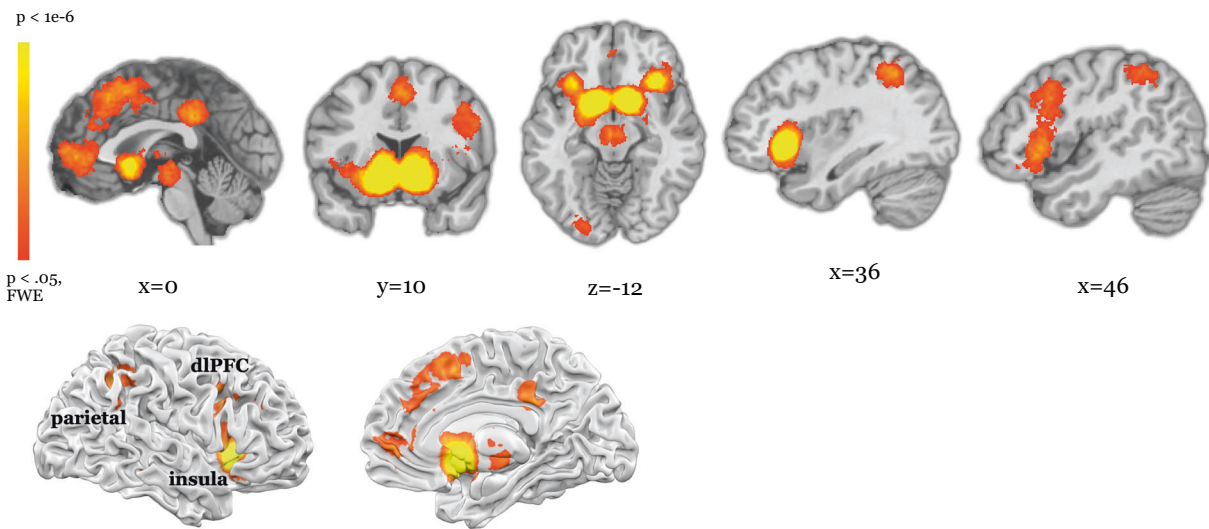
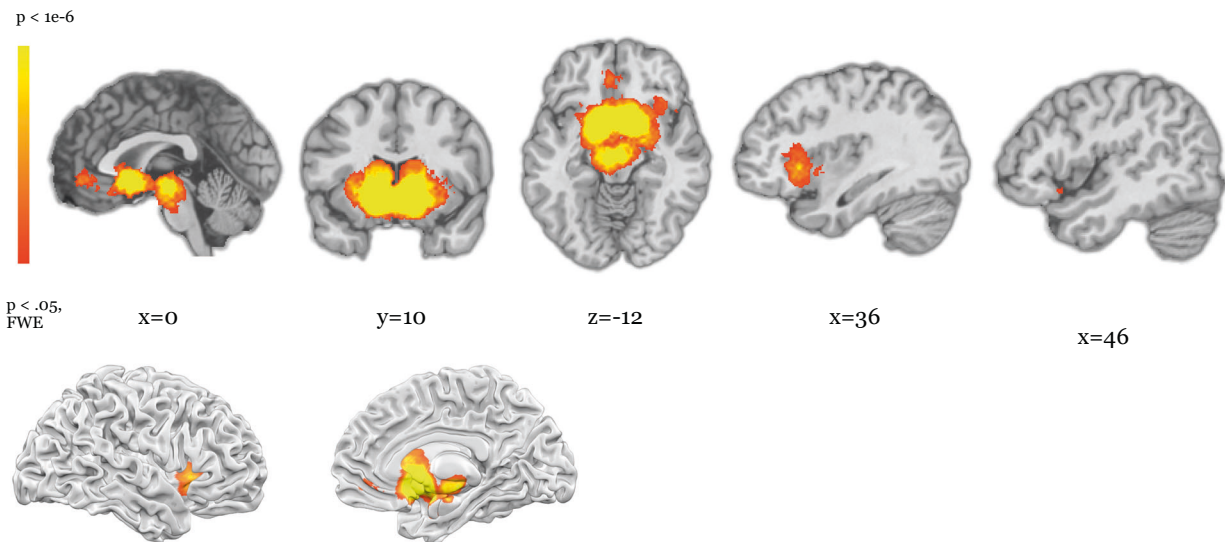


Fig. 4 Social and unsigned prediction errors. **A** Social PEs engaged medial PFC, dorsomedial PFC, dorsal and ventral striatum, and insula. **B** Unsigned PEs showed activity in the dorsomedial PFC and anterior cingulate, dorsal and ventral striatum, midbrain, insula, middle frontal gyrus, precentral gyrus and inferior frontal gyrus. **C** We also found relatively more activation for social PEs than non-social PEs in the anterior cingulate, ventromedial PFC, and dorsomedial PFC (orange). Regions including dorsal and ventral striatum, left insula, subgenual and posterior cingulate, showed more activity for non-social than social PEs (blue). **D** We computed the intersection between regions evincing PEs during social tasks, and those reflecting non-social PEs, and in particular, precision-weighted PEs. Regions including caudate, ventrolateral PFC, dorsomedial PFC, and insula appeared in the intersection between social and precision-weighted, non-social PEs.

A. PEs: Whole-brain analyses



B. PEs: ROI analyses



C. PEs in Whole-Brain Analyses > PEs in ROI Analyses

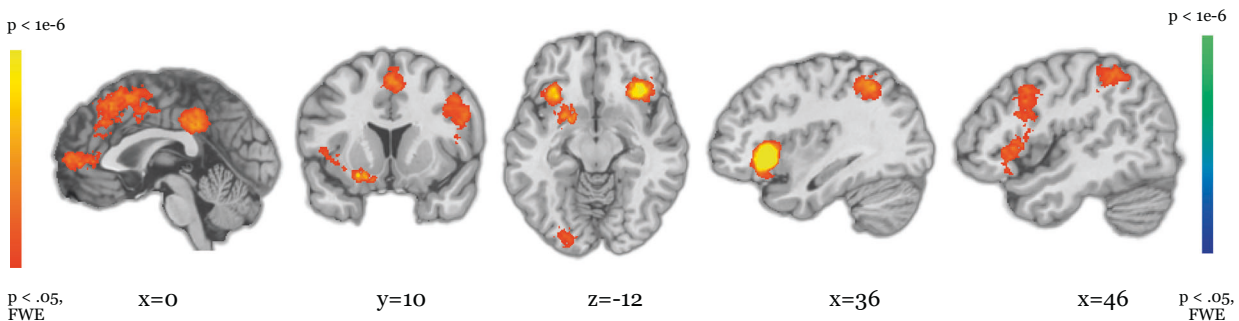


Fig. 5 Prediction errors from whole brain and region of interest analyses. **A** Results from whole brain analyses consistently reported PE signals in the dorsolateral prefrontal, parietal, and visual cortices, along with striatum, amygdala, anterior and posterior cingulate, insula, medial PFC and midbrain. **B** Studies that employed ROI masks that were often limited to the basal ganglia and midbrain. **C** The contrast of whole brain analyses compared to ROI analyses revealed activity in many regions, including medial and lateral PFC, insula, parietal cortex, temporal lobe and visual cortex.

out [27]. Here, we found domain-general precision-weighting had algorithmic and implementational overlap with social inference, consistent with the idea that social inferences tax the general inference machinery, rather than a separate social processing module. We did, however, find greater responses to social than non-social PE in the dmPFC (Fig. 4C), consistent with the engagement of this region during theory of mind tasks [56] and single unit recording [29]. It is possible that this region represents PEs specific to the social domain, although this was not clearly the case at the single neuron level [29]. Some theories of cognitive function and dysfunction posit domain-specific mechanisms [57]. Others hypothesize more domain-general processes [58–60]. The involvement of social versus non-social PE signals in some phenomenon of interest might serve a means of adjudicating.

Many of the extra-striatal PE signals we report may have been ignored because of the practice of a-priori ROI masking. The field had strong expectations of basal ganglia and midbrain PE based on the preclinical electrophysiology. Initially, it was important to confirm these signals in the human brain by focusing specifically on those regions. However, such an approach has failed to capitalize on one of the strengths of functional neuroimaging; namely that we can acquire an image of the whole brain every few seconds [61]. Analyses that explored PE signals outside of the narrow striatal field of view tended to report PEs in the lateral frontal, parietal, and visual cortices.

Summary

We believe our work has three main mechanistic implications:

1. There is a core, domain general circuit incorporating the striatum and insula, and likely midbrain, which signals PEs during perception, cognition, and action, with social agents as well as non-social tasks. This circuitry may serve as a locus of translation across species.
2. There are domain-specific and circumscribed PE mechanisms—for example in visual perceptual tasks, and social tasks. Focusing on social PEs may inform the social deficits observed in people with serious mental illnesses. For the visual, the interplay between perceptual PEs proper, and more general mechanisms may inform the mechanisms of perception, as well as perceptual aberrations in illness.
3. The practice of ROI masking, whilst well-grounded in monkey and more recently rodent work, has perhaps limited our inquiries into PE signaling in humans. The current novel finding that there are numerous cortical targets for general and specific error signals bodes well for mechanistic investigations using transcranial magnetic stimulation in human health and disease.

CONCLUSION

These results provide insights into animals, humans, and machines. Preclinical researchers might search for the more nuanced extra-striatal PEs we found, targeting homologous structures in animal brains. Indeed, this work has already begun [62]. Thus far, careful dissections of circuit mechanisms of PE have involved several brain regions [63]. Human fMRI of PE, including the present work, may help contextualize and expand this effort by providing whole brain insights. This must of course be coupled with a deeper inquiry into and appreciation of the mechanisms of the BOLD signal, which likely reflects local field potentials, and thus inputs to a region rather than spiking within it [64]. Combining incisive and precise recording and manipulation techniques along with BOLD measurements will be particularly revealing, and has been already [65, 66].

Human researchers might use these maps to choose tasks, analyses, or a priori circuits of interest to study, should they have

specific questions or suspect particular PE dysfunctions. Further, by delineating which algorithms might be implemented in the human brain, and how, our data may be relevant to the development of human-inspired artificial intelligence [67, 68]. More broadly, we answer critics of fMRI by offering concrete examples of functional imaging data informing models of cognitive function, proffering new testable predictions.

DATA AVAILABILITY

All maps featured (included in the figures and described in the text) are available on Neurovault (<https://neurovault.org/collections/IMXQLEGV/>). These may be used to generate region of interest masks for each feature, comparison, or conjunction. Tables of coordinates for each contrast and conjunction are available on the Open Science Framework (OSF, https://osf.io/6nuw7/?view_only=6fa6a080c3434409a07100f7c8088d87), as well as in supplementary information.

REFERENCES

1. Schultz W, Dayan P, Montague PR. A neural substrate of prediction and reward. *Science*. 1997;275:1593–9.
2. Pan WX, Schmidt R, Wickens JR, Hyland BI. Dopamine cells respond to predicted events during classical conditioning: evidence for eligibility traces in the reward-learning network. *J Neurosci*. 2005;25:6235–42.
3. Cohen JY, Haesler S, Vong L, Lowell BB, Uchida N. Neuron-type-specific signals for reward and punishment in the ventral tegmental area. *Nature*. 2012;482:85–8.
4. Zaghoul KA, Blanco JA, Weidemann CT, McGill K, Jaggi JL, Baltuch GH, et al. Human substantia nigra neurons encode unexpected financial rewards. *Science*. 2009;323:1496–9.
5. Garrison J, Erdeniz B, Done J. Prediction error in reinforcement learning: a meta-analysis of neuroimaging studies. *Neurosci Biobehav Rev*. 2013;37:1297–310.
6. Steinberg EE, Keiflin R, Boivin JR, Witten IB, Deisseroth K, Janak PH. A causal link between prediction errors, dopamine neurons and learning. *Nat Neurosci*. 2013;16:966–73.
7. Iglesias S, Mathys C, Brodersen KH, Kasper L, Piccirelli M, den Ouden HE, et al. Hierarchical prediction errors in midbrain and basal forebrain during sensory learning. *Neuron*. 2013;80:519–30.
8. Behrens TE, Hunt LT, Woolrich MW, Rushworth MF. Associative learning of social value. *Nature*. 2008;456:245–9.
9. Brown M, Kuperberg GR. A hierarchical generative framework of language processing: linking language perception, interpretation, and production abnormalities in schizophrenia. *Front Hum Neurosci*. 2015;9:643.
10. Corlett PR, Aitken MR, Dickinson A, Shanks DR, Honey GD, Honey RA, et al. Prediction error during retrospective reevaluation of causal associations in humans: fMRI evidence in favor of an associative model of learning. *Neuron*. 2004;44:877–88.
11. Kober H, Wager TD. Meta-analysis of neuroimaging data. *Wiley Interdiscip Rev: Cogn Sci*. 2010;1:293–300.
12. Schenk LA, Sprenger C, Onat S, Colloca L, Büchel C. Suppression of striatal prediction errors by the prefrontal cortex in placebo hypoalgesia. *J Neurosci*. 2017;37:9715–23.
13. Friston KJ, Worsley KJ, Frackowiak RS, Mazziotta JC, Evans AC. Assessing the significance of focal activations using their spatial extent. *Hum Brain Mapp*. 1994;1:210–20.
14. Friston KJ, Holmes AP, Price CJ, Büchel C, Worsley KJ. Multisubject fMRI studies and conjunction analyses. *Neuroimage*. 1999;10:385–96.
15. Levy DJ, Glimcher PW. The root of all value: a neural common currency for choice. *Curr Opin Neurobiol*. 2012;22:1027–38.
16. Friston KJ, Shiner T, FitzGerald T, Galea JM, Adams R, Brown H, et al. Dopamine, affordance and active inference. *PLoS Comput Biol*. 2012;8:e1002327.
17. Dickinson A, Balliène BW. The Role of Learning in the Operation of Motivational Systems, in Stevens' Handbook of Experimental Psychology. 2002.
18. Ostlund SB, Balleine BW. Orbitofrontal cortex mediates outcome encoding in Pavlovian but not instrumental conditioning. *J Neurosci*. 2007;27:4819–25.
19. Rich EL, Wallis JD. Medial-lateral organization of the orbitofrontal cortex. *J Cogn Neurosci*. 2014;26:1347–62.
20. Panayi MC, Killcross S. The role of the rodent lateral orbitofrontal cortex in simple Pavlovian cue-outcome learning depends on training experience. *Cereb Cortex Commun*. 2021;2:tgab010.
21. Ma C, Jean-Richard-Dit-Bressel P, Roughley S, Vissel B, Balleine BW, Killcross S, et al. Medial orbitofrontal cortex regulates instrumental conditioned punishment, but not Pavlovian conditioned fear. *Cereb Cortex Commun*. 2020;1:tgaa039.
22. Schmack K, Bosc M, Ott T, Sturgill JF, Kepecs A. Striatal dopamine mediates hallucination-like perception in mice. *Science*. 2021; 372. <https://doi.org/10.1126/science.abf4740>.

23. Friston KJ. The free-energy principle: a rough guide to the brain? *Trends Cogn Sci*. 2009;13:293–301.
24. Pearce JM, Hall G. A model for Pavlovian learning: variations in the effectiveness of conditioned but not of unconditioned stimuli. *Psychol Rev*. 1980;87:532–52.
25. Mackintosh NJ. A theory of attention: variations in the associability of stimuli with reinforcement. *Psychological Rev*. 1975;82:pp–298.
26. Adolphs R. Social cognition and the human brain. *Trends Cogn Sci*. 1999;3:469–79.
27. Lockwood PL, Apps MAJ, Chang SWC. Is there a ‘social’ brain? implementations and algorithms. *Trends Cogn Sci*. 2020;24:802–13.
28. Zaki J, Kallman S, Wimmer GE, Ochsner K, Shohamy D. Social cognition as reinforcement learning: feedback modulates emotion inference. *J Cogn Neurosci*. 2016;28:1270–82.
29. Jamali M, Grannan BL, Fedorenko E, Saxe R, Báez-Mendoza R, Williams ZM. Single-neuronal predictions of others’ beliefs in humans. *Nature*. 2021; 610–4.
30. Fouragnan E, Retzler C, Philiastides MG. Separate neural representations of prediction error valence and surprise: evidence from an fMRI meta-analysis. *Hum Brain Mapp*. 2018;39:2887–906.
31. D’Astolfo L, Rief W. Learning about expectation violation from prediction error paradigms—A meta-analysis on brain processes following a prediction error. *Front Psychol*. 2017;8:1253.
32. Chase HW, Kumar P, Eickhoff SB, Dombrowski AY. Reinforcement learning models and their neural correlates: an activation likelihood estimation meta-analysis. *Cogn, Affect, Behav Neurosci*. 2015;15:435–59.
33. Sharpe MJ, Chang CY, Liu MA, Batchelor HM, Mueller LE, Jones JL, et al. Dopamine transients are sufficient and necessary for acquisition of model-based associations. *Nat Neurosci*. 2017;20:735–42.
34. Friston K. A theory of cortical responses. *Philos Trans R Soc Lond B Biol Sci*. 2005;360:815–36.
35. Rao RP, Ballard DH. Predictive coding in the visual cortex: a functional interpretation of some extra-classical receptive-field effects. *Nat Neurosci*. 1999;2:79–87.
36. Haber SN, Fudge JL, McFarland NR. Striatonigrostriatal pathways in primates form an ascending spiral from the shell to the dorsolateral striatum. *J Neurosci*. 2000;20:2369–82.
37. Rogan MT, Leon KS, Perez DL, Kandel ER. Distinct neural signatures for safety and danger in the amygdala and striatum of the mouse. *Neuron*. 2005;46:309–20.
38. Josselyn SA, Falls WA, Gwartz JC, Pistell P, Davis M. The nucleus accumbens is not critically involved in mediating the effects of a safety signal on behavior. *Neuropsychopharmacology*. 2005;30:17–26.
39. Menegas W, Akiti K, Amo R, Uchida N, Watabe-Uchida M. Dopamine neurons projecting to the posterior striatum reinforce avoidance of threatening stimuli. *Nat Neurosci*. 2018;21:1421–30.
40. Seymour B, Daw N, Dayan P, Singer T, Dolan R. Differential encoding of losses and gains in the human striatum. *J Neurosci*. 2007;27:4826–31.
41. Lammel S, Lim BK, Ran C, Huang KW, Betley MJ, Tye KM, et al. Input-specific control of reward and aversion in the ventral tegmental area. *Nature*. 2012;491:212–7.
42. Belova MA, Paton JJ, Morrison SE, Salzman CD. Expectation modulates neural responses to pleasant and aversive stimuli in primate amygdala. *Neuron*. 2007;55:970–84.
43. Belova MA, Paton JJ, Salzman CD. Moment-to-moment tracking of state value in the amygdala. *J Neurosci*. 2008;28:10023–30.
44. Morrison SE, Salzman CD. Re-valuing the amygdala. *Curr Opin Neurobiol*. 2010;20:221–30.
45. Paton JJ, Belova MA, Morrison SE, Salzman CD. The primate amygdala represents the positive and negative value of visual stimuli during learning. *Nature*. 2006;439:865–70.
46. Sangha S, Chadick JZ, Janak PH. Safety encoding in the basal amygdala. *J Neurosci*. 2013;33:3744–51.
47. Shabel SJ, Janak PH. Substantial similarity in amygdala neuronal activity during conditioned appetitive and aversive emotional arousal. *Proc Natl Acad Sci USA*. 2009;106:15031–6.
48. Roesch MR, Calu DJ, Esber GR, Schoenbaum G. Neural correlates of variations in event processing during learning in basolateral amygdala. *J Neurosci*. 2010;30:2464–71.
49. Lisman JE, Grace AA. The hippocampal-VTA loop: controlling the entry of information into long-term memory. *Neuron*. 2005;46:703–13.
50. Preusschoff K, Mohr PN, Hsu M. Decision making under uncertainty. *Front Neurosci*. 2013;7:218.
51. Schultz W, Preusschoff K, Camerer C, Hsu M, Fiorillo CD, Tobler PN, et al. Explicit neural signals reflecting reward uncertainty. *Philos Trans R Soc Lond B Biol Sci*. 2008;363:3801–11.
52. Preusschoff K, Bossaerts P. Adding prediction risk to the theory of reward learning. *Ann N. Y Acad Sci*. 2007;1104:135–46.
53. Powers AR, Mathys C, Corlett PR. Pavlovian conditioning-induced hallucinations result from overweighting of perceptual priors. *Science*. 2017;357:596–600.
54. Levorsen M, Ito A, Suzuki S, Izuma K. Testing the reinforcement learning hypothesis of social conformity. *Hum Brain Mapp*. 2020.
55. Davis T, LaRocque KF, Mumford JA, Norman KA, Wagner AD, Poldrack RA. What do differences between multi-voxel and univariate analysis mean? How subject-, voxel-, and trial-level variance impact fMRI analysis. *Neuroimage*. 2014;97:271–83.
56. Denny BT, Kober H, Wager TD, Ochsner KN. A meta-analysis of functional neuroimaging studies of self- and other judgments reveals a spatial gradient for mentalizing in medial prefrontal cortex. *J Cogn Neurosci*. 2012;24:1742–52.
57. Raihani NJ, Bell V. An evolutionary perspective on paranoia. *Nat Hum Behav*. 2019;3:114–21.
58. Reed EJ, Uddenberg S, Suthaharan P, Mathys CD, Taylor JR, Groman SM, et al. Paranoia as a deficit in non-social belief updating. *Elife*. 2020; 9:e56345. <https://doi.org/10.7554/eLife.56345>.
59. Suthaharan P, Reed EJ, Leptourgos P, Kenney JG, Uddenberg S, Mathys CD, et al. Paranoia and belief updating during the COVID-19 crisis. *Nat Hum Behav*. 2021;5:1190–202.
60. Feeney EJ, Groman SM, Taylor JR, Corlett PR. Explaining delusions: reducing uncertainty through basic and computational neuroscience. *Schizophr Bull*. 2017;43:263–72.
61. Moeller S, Yacoub E, Olman CA, Auerbach E, Strupp J, Harel N, et al. Multiband multislice GE-EPI at 7 tesla, with 16-fold acceleration using partial parallel imaging with application to high spatial and temporal whole-brain fMRI. *Magn Reson Med*. 2010;63:1144–53.
62. Millard SJ, Bearden CE, Karlsgodt KH, Sharpe MJ. The prediction-error hypothesis of schizophrenia: new data point to circuit-specific changes in dopamine activity. *Neuropsychopharmacology*. 2021. <https://doi.org/10.1038/s41386-021-01188-y>.
63. Watabe-Uchida M, Eshel N, Uchida N. Neural circuitry of reward prediction error. *Annu Rev Neurosci*. 2017;40:373–94.
64. Logothetis NK, Pauls J, Augath M, Trinath T, Oeltermann A. Neurophysiological investigation of the basis of the fMRI signal. *Nature*. 2001;412:150–7.
65. Ferenczi EA, Zalocusky KA, Liston C, Grosenick L, Warden MR, Amatya D, et al. Prefrontal cortical regulation of brainwide circuit dynamics and reward-related behavior. *Science*. 2016;351:aac9698.
66. Lohani S, Poplawsky AJ, Kim SG, Moghaddam B. Unexpected global impact of VTA dopamine neuron activation as measured by opto-fMRI. *Mol Psychiatry*. 2017;22:585–94.
67. Richards BA, Lillcrap TP, Beaudoin P, Bengio Y, Bogacz R, Christensen A, et al. A deep learning framework for neuroscience. *Nat Neurosci*. 2019;22:1761–70.
68. Marblestone AH, Wayne G, Kording KP. Toward an integration of deep learning and neuroscience. *Front Comput Neurosci*. 2016;10:94.

FUNDING

JAM and HK were supported by R01 DA043690. PRC was supported by R21MH116258 and R01MH12887. This work was supported by the Yale University Department of Psychiatry, the Connecticut Mental Health Center (CMHC) and Connecticut State Department of Mental Health and Addiction Services (DMHAS). The funders had no role in study design, data collection and analysis, decision to publish or preparation of the manuscript.

COMPETING INTERESTS

The authors declare no competing interests.

ADDITIONAL INFORMATION

Supplementary information The online version contains supplementary material available at <https://doi.org/10.1038/s41386-021-01264-3>.

Correspondence and requests for materials should be addressed to Philip R. Corlett or Hedy Kober.

Reprints and permission information is available at <http://www.nature.com/reprints>

Publisher’s note Springer Nature remains neutral with regard to jurisdictional claims in published maps and institutional affiliations.